nature climate change

LETTERS

PUBLISHED ONLINE: 22 FEBRUARY 2016 | DOI: 10.1038/NCLIMATE2935

Climate and health impacts of US emissions reductions consistent with 2 °C

Drew T. Shindell[1]*, Yunha Lee[1] and Greg Faluvegi[2]

An emissions trajectory for the US consistent with 2 °C warming would require marked societal changes, making it crucial to understand the associated benefits. Previous studies have examined technological potentials and implementation costs[1,2] and public health benefits have been quantified for less-aggressive potential emissions-reduction policies (for example, refs 3,4), but researchers have not yet fully explored the multiple benefits of reductions consistent with 2 °C. We examine the impacts of such highly ambitious scenarios for clean energy and vehicles. US transportation emissions reductions avoid ~0.03 °C global warming in 2030 (0.15 °C in 2100), whereas energy emissions reductions avoid ~0.05–0.07 °C 2030 warming (~0.25 °C in 2100). Nationally, however, clean energy policies produce climate disbenefits including warmer summers (although these would be eliminated by the remote effects of similar policies if they were undertaken elsewhere). The policies also greatly reduce damaging ambient particulate matter and ozone. By 2030, clean energy policies could prevent ~175,000 premature deaths, with ~22,000 (11,000–96,000; 95% confidence) fewer annually thereafter, whereas clean transportation could prevent ~120,000 premature deaths and ~14,000 (9,000–52,000) annually thereafter. Near-term national benefits are valued at ~US$250 billion (140 billion to 1,050 billion) per year, which is likely to exceed implementation costs. Including longer-term, worldwide climate impacts, benefits roughly quintuple, becoming ~5–10 times larger than estimated implementation costs. Achieving the benefits, however, would require both larger and broader emissions reductions than those in current legislation or regulations.

The US has pledged to markedly reduce emissions that cause warming but has left many details to be determined later. We construct emission scenarios for the primary sectors contributing to climate change and air quality degradation. We then model the effects of those to quantify the human health benefits and the near- and long-term climate impacts both locally and globally. Finally, we analyse the economic valuation of those benefits and compare with costs.

To derive 2030 emissions, we use a constant rate of decrease between 2015 and 2050 (2.7% yr^{-1}; see Supplementary Information) that leads to the 80% reduction relative to approximate current emissions targeted for 2050 and consistent with 2 °C warming. Under this scenario, emissions need to be ~40% below current levels in 2030, or ~4,000 $TgCO_2e\ yr^{-1}$, and ~62% below baseline 2030 emissions. This is similar to a five-year extrapolation of the 2015 US–China agreement under which the US agreed to reductions relative to 2005 of 17% by 2020 and 28% by 2025, and to previous analysis of US decarbonization[2]. We create a 'clean transportation' scenario under which surface transport emissions are reduced by 75% and a 'clean energy' scenario reducing energy sector emissions by 63% relative to the baseline. We use Representative Concentration Pathway 8.5 (RCP8.5) for the baseline, and for all emissions under these scenarios except for these US sectors, for which all pollutants are reduced uniformly. These scenarios are beyond announced policies, but technically feasible and in accord with other proposals (see Supplementary Information). The policies strongly reduce CO_2 emissions from both sectors, with additional substantial reductions in methane, SO_2 and NO_x emissions from energy and CO and NO_x from surface transportation (Supplementary Table 1).

These scenarios were used to drive simulations of atmospheric composition using two models. In 2030, the clean energy policy causes positive global mean aerosol radiative forcing owing primarily to reduced sulphate, but negative forcing through reduced ozone and methane, so that the net total forcing is almost identical to the forcing from CO_2 alone (~−50 mW m^{-2}; Supplementary Table 2). In the clean transportation scenario, there is a reduction in ozone but an increase in methane (due to reduced oxidation), and very small positive aerosol forcings. Hence, again the net total forcing is similar to the CO_2 forcing at the global scale (~−30 mW m^{-2}). The CO_2 forcing increases to −118 mW m^{-2} at 2050 and −213 mW m^{-2} at 2100 for energy, and to −76 and −136 mW m^{-2} for transportation at those times, respectively (see Supplementary Information). Hence, for global mean surface temperature, both policies are beneficial at all timescales.

Although both policies lead to reductions in global mean radiative forcing, local values can be quite different from the global mean for most of the near-term climate forcers (defined here as methane, aerosols and ozone-related species). In particular, the large decreases in SO_2 emissions under the energy policy scenario lead to very strong positive aerosol radiative forcing over the US (Supplementary Table 3). Aerosol radiative forcing exceeds 300 mW m^{-2} over much of the US, largely owing to direct forcing in the east and to aerosol–cloud forcing in the Mountain West (Fig. 1). The direct forcing is greatest in the east because most of the sulphur dioxide emissions are located there, whereas the aerosol–cloud response is largest in the Mountain West because clouds are much more sensitive to aerosol changes at the lower aerosol concentrations found in that comparatively unpolluted region (for example, ref. 7). This positive aerosol forcing dominates the net forcing in 2030 over the US (Fig. 1 and Supplementary Table 3). The US radiative forcing under the transportation policy shows similar patterns, but with reduced magnitude (Fig. 1). In this case, net aerosol forcing is positive owing to reductions in emissions of organic carbon and NO_x, the latter leading to reductions in nitrate aerosols (see Supplementary Information). Over time, however, the influence of CO_2 grows, so that net US radiative forcing becomes negative under

[1]Nicholas School of the Environment, Duke University, Durham, North Carolina 27708, USA. [2]NASA Goddard Institute for Space Studies, New York, New York 10025, USA. *e-mail: drew.shindell@duke.edu

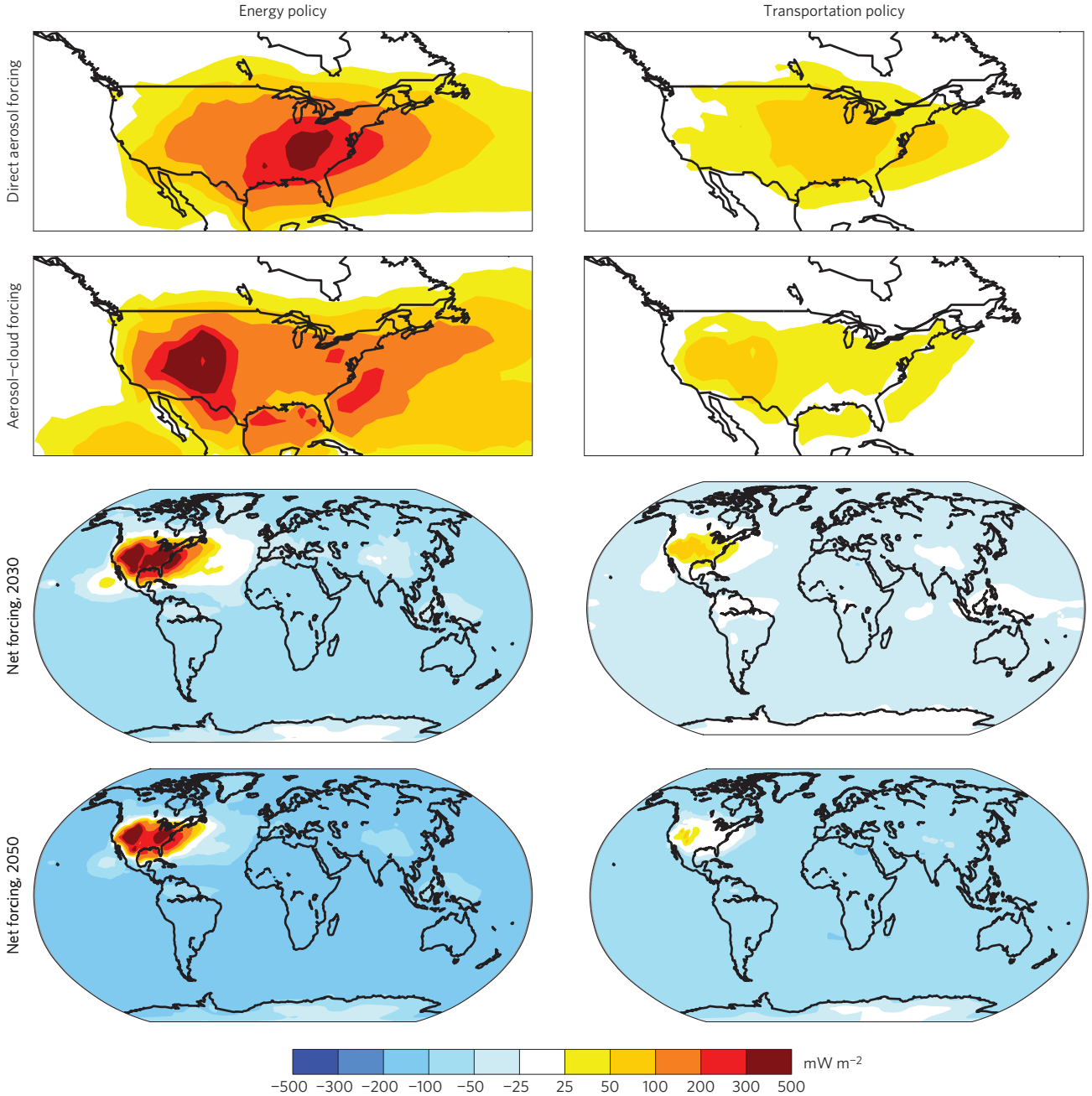

Figure 1 | Radiative forcing due to clean energy and clean transportation. Values are shown for 2030 for the energy (left column) and transportation (right column) policy scenarios relative to the baseline for aerosols (top two rows) and net forcing in 2030 and 2050 (bottom two rows) based on the model version incorporating mass-based aerosols (see Supplementary Fig. 1 for the model incorporating aerosol microphysics). Net forcing includes aerosols, ozone (which is small compared with aerosols), CH_4 and CO_2 (which are fairly uniform). Coloured values are statistically significant (95% based on interannual variability; Figs 1–4).

either policy relative to the baseline (Fig. 2). The transition takes place earlier in the case of the transportation policy than the energy policy in both models. Using detailed aerosol microphysics, the transitions occur in 2024 and 2069 for transportation and energy policies, respectively, whereas using the mass-based aerosol model they take place in 2035 and 2089.

We examine the climate response in 200-year coupled ocean–atmosphere simulations comparing a 2030 control with an experiment decreasing US energy sector emissions. These long equilibrium simulations provide statistically significant results. Transient response at 2030 would be ∼15–20% less in magnitude (based on our model). Global mean temperatures decrease by ∼0.05 °C, but annual average temperatures over much of the US barely change (Fig. 3). During the boreal summer, the contiguous US warms owing to the reduced sulphate, which causes especially large positive forcing during this season. Most areas outside the US experience cooling due to reduced CO_2, but several other Northern Hemisphere mid-latitude and Arctic regions also see modest summer warming, consistent with the enhanced sensitivity of those two latitude bands to Northern Hemisphere mid-latitude forcing[8]. Although regional responses to aerosol forcing vary substantially across models[5], these results highlight the potential for near-term local climate disbenefits due to clean energy policies, highlighting the value of international cooperation to reduce both near-term climate forcers and CO_2.

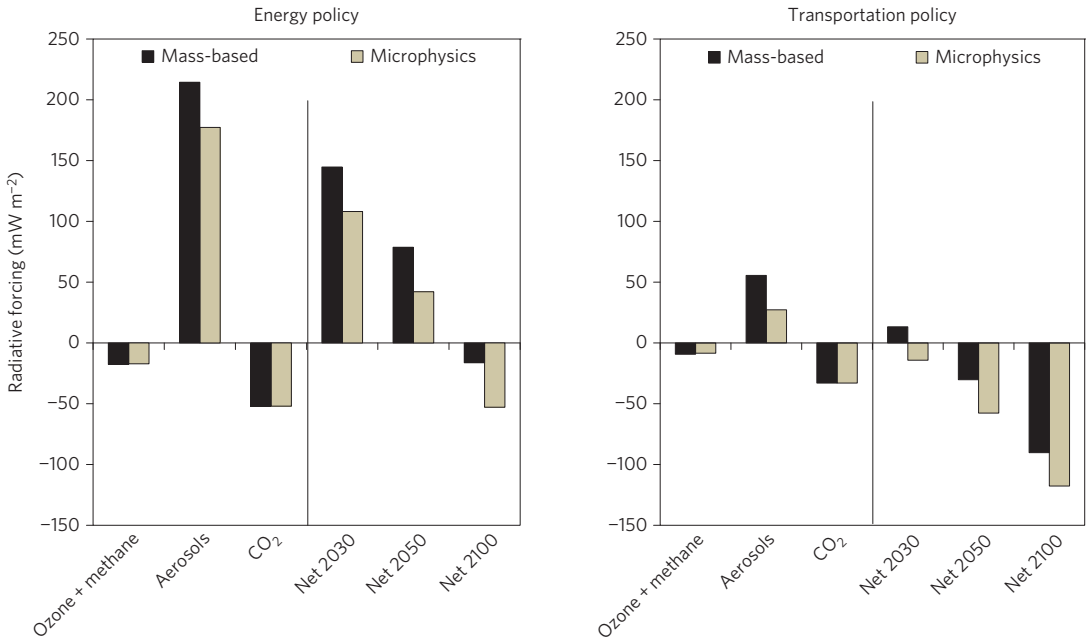

Figure 2 | Radiative forcing over the United States due to the two policies. Values are given for both aerosol models by component at 2030 and the net is given versus time. Values greater than ~3 mW m^{-2} are statistically significant.

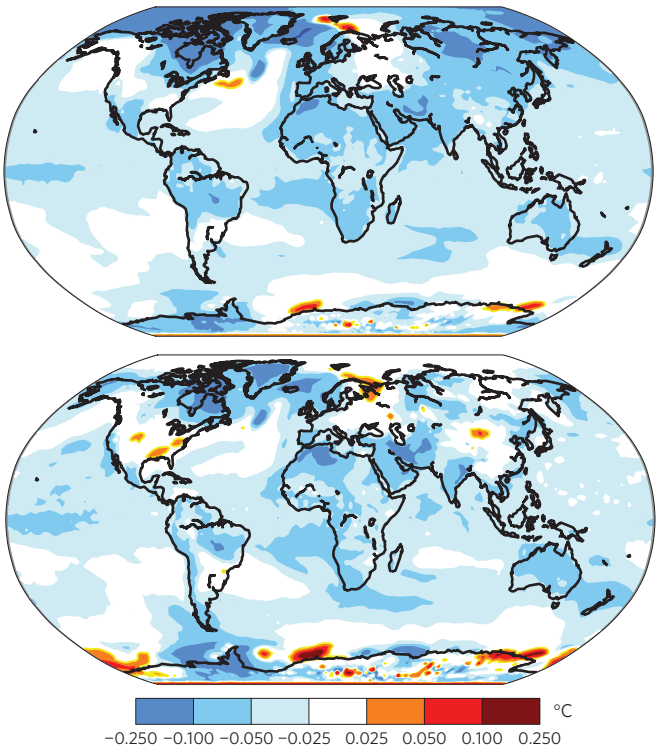

Figure 3 | Equilibrium annual (top) and boreal summer (bottom) average surface temperature response to the clean energy scenario. Coloured values are significant in the contiguous US states and most tropical and mid-latitude areas whereas only absolute values greater than about 0.1 °C are significant at high latitudes.

As climate simulations are computationally expensive, we simply estimated temperature responses for other times and for the transportation scenario using the time-dependent response to radiative forcing from the Hadley Centre model[6]. In 2030, the clean transportation scenario has ~0.03 °C less warming globally whereas the clean energy scenario has ~0.07 °C less (a value slightly larger than that obtained in our climate simulations owing to the higher sensitivity in the Hadley Centre model relative to the GISS (Goddard Institute for Space Studies) model). These benefits increase to ~0.15 °C and ~0.25 °C in 2100 for these cases, respectively, assuming constant post-2030 CO_2 emissions. As with radiative forcing the values are small relative to projected baseline warming but are substantial considering they stem from emission controls within a single nation and sector.

Reductions in surface particulate matter with a diameter smaller than 2.5 μm ($PM_{2.5}$), which is robustly linked to adverse human health impacts (for example, ref. 9), are greatest over the eastern US where sulphur dioxide emissions decrease the most for the energy scenario (Fig. 4). Reductions attributable to clean transportation maximize in the upper Midwest where large ammonia emissions due to agriculture and small SO_2 emissions lead to NO_x emissions readily forming nitrate.

We calculated the effects of these $PM_{2.5}$ changes and ozone changes on human health based on concentration–response functions (CRFs) from epidemiological studies, with CRF variants used to characterize uncertainties. The health impacts broadly follow the location of the $PM_{2.5}$ changes, although population density also influences results (Fig. 4). Differences between the two aerosol models are relatively small for the energy scenario. They are large for the transportation scenario, reflecting the importance of the nitrate response to NO_x (included in the mass-based model but not in the microphysics model). Nonetheless, variation across CRFs seems to exceed that from physical uncertainties (here and, for example, in ref. 10).

Roughly 22,000 (10,000–96,000) premature deaths are prevented annually under the clean energy scenario and ~14,000 (9,000–52,000) for clean transportation by 2030. Totals over 2015–2030 are ~175,000 and ~120,000, respectively for CRF_{base}. Uncertainties include intermodel composition differences and CRF variations and are dominated by $PM_{2.5}$ CRFs. We assume that these approximately represent 95% confidence intervals. Ozone decreases are responsible for ~4,000 annually avoided premature deaths for energy and ~5,000 for transport, with their relative importance highly sensitive to the $PM_{2.5}$ methodology. For $PM_{2.5}$, 89–91% of

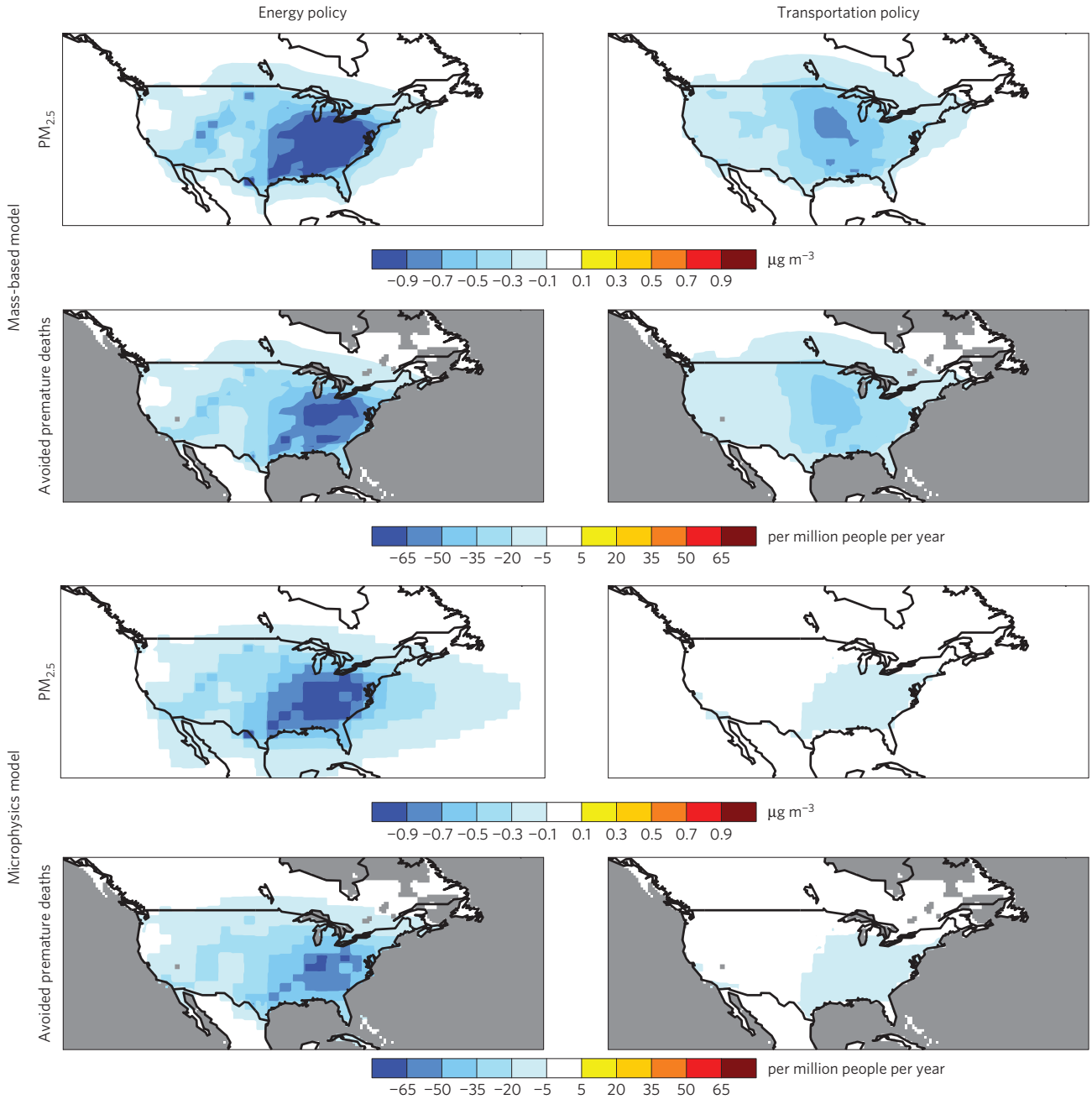

Figure 4 | Annual average change in surface $PM_{2.5}$ and $PM_{2.5}$-related mortalities. Values are presented for the two policies and the two models. Coloured values are statistically significant. Eastern US $PM_{2.5}$ reductions in the energy policy case are between 1 and 2 μg m^{-3}. Health values are for the sum of all causes examined here and use CRF_{base}.

benefits are within the US, whereas only 26–33% of ozone-related benefits occur domestically (Supplementary Fig. 2). Of the total $PM_{2.5}$ plus ozone impacts, ∼3–4% are in Canada and ∼1–2% in Mexico.

We monetized these health benefits and calculated societal welfare more broadly using the Social Cost of Atmospheric Release (SCAR), which includes climate and air quality benefits[11]. The monetized air quality benefits within the SCAR are globally representative, and are ∼20–25% less than those found in these calculations (consistent with relatively high North American incomes). SCAR valuation with mid-range (3%) discounting is ∼US$800 billion (400 billion to 1,700 billion) for clean energy and ∼US$400 billion (200 billion to 1,000 billion) for clean transportation (Fig. 5). Both the total valuation and the fraction attributable to the direct effects of air quality on human health vary with the discount rate. In comparison, valuation using the US Government's Social Cost of Carbon[12] that monetizes reductions in CO_2 alone is ∼US$210 billion and ∼US$140 billion, respectively, for 3% discounting. Hence, that methodology (and most climate policy analyses, as these typically neglect air quality valuation[13]) encompasses only ∼1/3–1/4 of the benefits found here and only those occurring over long timescales, implying an overly strong mismatch between near-term implementation costs and the timing of benefits.

Premature deaths are the only air quality impact valued here, but effects on medical spending and worker productivity can be quite large[14]. For example, based on the ratio of impacts in previous analyses[15], the clean energy and transportation policies together could prevent ∼29,000 asthma attacks in children under 18

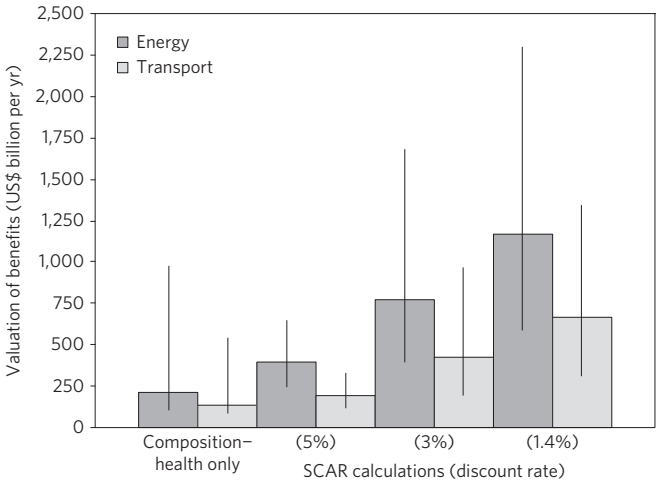

Figure 5 | Valuation of worldwide societal benefits from the two policies. Values are human health benefits due to improved air quality based on the composition–climate modelling (leftmost pair of bars) and valuation of air quality and climate benefits using the SCAR metric (right three pairs of bars). Uncertainty in the composition–health impacts stems from the various CRFs examined here, whereas uncertainty in the SCAR valuation incorporates the uncertainty in the CRF_{base} case relative risk estimates alone for composition–health, along with multiple uncertainties related to climate and economic projections (95% confidence).

requiring emergency room visits and ~15,000,000 lost adult work days each year.

Although differences in the relative changes of various pollutants complicate any comparison with previous studies, it seems that our results are broadly consistent with other work using more detailed scenarios (see Supplementary Information). It is hence useful to compare our benefits with estimated costs. The EPA (Environmental Protection Agency) estimated implementation costs for the proposed Clean Power Plan of US$7 billion to US$9 billion (ref. 16). This plan achieves roughly half of the CO_2 emission reductions of our energy scenario. Although costs might increase as reductions deepen, this suggests that at least for the first half of the energy sector emissions reductions the net societal benefits are roughly 20–80 times the implementation costs. Furthermore, an analysis with emissions reductions similar to ours[2] estimated 2030 economy-wide additional costs of ~US$100 billion to US$210 billion. Another study found that provision of all energy by renewables could leave energy costs virtually unchanged[1]. Hence, benefits seem to outweigh costs by at least a factor of 5–10 even for deep decarbonization with costs more than tenfold greater than the Clean Power Plan. The air quality-related health benefits are realized almost immediately and are primarily domestic, so that the near-term national gains alone (Fig. 5) are also larger than the implementation costs in contrast to the temporal and spatial mismatches between emissions controls and benefits typical of climate policies.

Implementation is nonetheless extremely challenging. Most benefits would accrue to society at large whereas businesses that could face economic losses would not directly benefit from decreased emissions. These misaligned economic incentives between the welfare of individual companies and that of society at large create substantial implementation barriers. Internalizing environmental damages within the economic system, for example, by means of damage recovery fees or avoidance credits, is the most obvious way to remove these barriers to achieving net societal benefits.

Methods

Methods and any associated references are available in the online version of the paper.

Received 28 September 2015; accepted 13 January 2016; published online 22 February 2016

References

1. Delucchi, M. A. & Jacobson, M. Z. Providing all global energy with wind, water, and solar power, part II: reliability, system and transmission costs, and policies. *Energy Policy* **39,** 1170–1190 (2011).
2. Williams, J. H. *et al*. *The US Report of the Deep Decarbonization Pathways Project* (Sustainable Development Solutions Network and the Institute for Sustainable Development and International Relations, 2014).
3. Thompson, T. M., Rausch, S., Saari, R. K. & Selin, N. E. A systems approach to evaluating the air quality co-benefits of US carbon policies. *Nature Clim. Change* **4,** 917–923 (2014).
4. Driscoll, C. T. *et al*. US power plant carbon standards and clean air and health co-benefits. *Nature Clim. Change* **5,** 535–540 (2015).
5. Shindell, D. T., Faluvegi, G., Rotstayn, L. & Milly, G. Spatial patterns of radiative forcing and surface temperature response. *J. Geophys. Res.* **120,** 5385–5403 (2015).
6. Boucher, O., Friedlingstein, P., Collins, B. & Shine, K. P. The indirect global warming potential and global temperature change potential due to methane oxidation. *Environ. Res. Lett.* **4,** 044007 (2009).
7. Gultepe, I. & Isaac, G. A. Scale effects on averaging cloud droplet and aerosol number concentrations: observations and models. *J. Clim.* **12,** 1268–1279 (1999).
8. Shindell, D. & Faluvegi, G. Climate response to regional radiative forcing during the 20th century. *Nature Geosci.* **2,** 294–300 (2009).
9. Lim, S., Vos, T. & Flaxman, A. A comparative risk assessment of burden of disease and injury attributable to 67 risk factors and risk factor clusters in 21 regions, 1990–2010: a systematic analysis for the Global Burden of Disease Study 2010. *Lancet* **380,** 2224–2260 (2012).
10. Anenberg, S. C. *et al*. Global air quality and health co-benefits of mitigating near-term climate change through methane and black carbon emission controls. *Environ. Health Perspect.* **120,** 831–839 (2012).
11. Shindell, D. The social cost of atmospheric release. *Climatic Change* **130,** 313–326 (2015).
12. US Government *Technical Update of the Social Cost of Carbon for Regulatory Impact Analysis Under Executive Order 12866* (Interagency Working Group on Social Cost of Carbon, 2013).
13. Nemet, G., Holloway, T. & Meier, P. Implications of incorporating air-quality co-benefits into climate change policymaking. *Environ. Res. Lett.* **5,** 014007 (2010).
14. Saari, R. K., Selin, N. E., Rausch, S. & Thompson, T. M. A self-consistent method to assess air quality co-benefits from U.S. climate policies. *J. Air Waste Manage. Assoc.* **65,** 74–89 (2015).
15. Fann, N. *et al*. Estimating the national public health burden associated with exposure to ambient $PM_{2.5}$ and ozone. *Risk Anal.* **32,** 81–95 (2012).
16. US EPA *Clean Power Plan Fact Sheet* (US Environmental Protection Agency, 2014); http://www2.epa.gov/sites/production/files/2014-06/documents/20140602fs-important-numbers-clean-power-plan.pdf

Acknowledgements

We thank K. Riahi and S. Rao from IIASA for providing information regarding MESSAGE RCP8.5 emissions. We thank NASA's Applied Science Program and the US Department of Transportation's Research and Innovation Technology Administration for financial support along with the NASA High-End Computing Program through the NASA Center for Climate Simulation at Goddard Space Flight Center for computational resources.

Author contributions

D.T.S. conceived the project; G.F. performed the simulations with the model incorporating mass-based aerosols; Y.L. performed those with the model incorporating aerosol microphysics. D.T.S. wrote the paper, with all authors providing input.

Additional information

Supplementary information is available in the online version of the paper. Reprints and permissions information is available online at www.nature.com/reprints. Correspondence and requests for materials should be addressed to D.T.S.

Competing financial interests

The authors declare no competing financial interests.

Methods

Experimental design. Simulations used the version of the GISS (Goddard Institute for Space Studies) ModelE2 used for the Coupled Model Intercomparison Project Phase 5 (CMIP5) and the Atmospheric Chemistry and Climate Model Intercomparison Project (ACCMIP; refs 17,18). Ocean conditions (sea-surface temperature and sea-ice cover) were prescribed at seasonally varying values for 2030 from our previous RCP8.5 simulations for radiative forcing and pollutant modelling. Forty-five-year simulations were performed with fixed ocean conditions but allowing atmospheric and land-surface responses, producing the Effective Radiative Forcing (ERF), and analyses use the last 40 years of these simulations for most forcing diagnostics. Aerosol–cloud forcings were not statistically significant, however, leading us to instead diagnose those from additional simulations with fixed meteorology (and therefore greatly reduced noise, but excluding cloud-lifetime changes). Those aerosol cloud–albedo forcings are based on the last 9 years of 10-year simulations. Although incomplete compared with the full ERF, this has provided a fairly good approximation of the global mean total in other cases (for example, the pre-industrial to present day cloud albedo forcing is $-0.58\ \mathrm{W\,m^{-2}}$ whereas the ERF-minus-direct aerosol forcing is $-0.61\ \mathrm{W\,m^{-2}}$ (ref. 19)). Radiative forcing due to methane changes is calculated over the last 10 years of the longer simulations. The impact of CO_2 changes is calculated using an offline set of analytic equations representing the carbon cycle[20], with CO_2 reductions imposed linearly from 2010 to 2030. Statistical analyses of the model are based on interannual variability and all confidence levels are 95%.

The most uncertain driver of climate forcing since the pre-industrial is aerosols[21]. Hence, we performed simulations using two very distinct representations of aerosols within the same host climate model. The first is the default aerosol model used in GISS CMIP5 simulations, a relatively simple mass-based aerosol scheme under which aerosols are assumed to be externally mixed and size information is prescribed[17]. The second is the TwO-Moment Aerosol Sectional (TOMAS) aerosol microphysics model, which predicts aerosol number and mass size distributions by computing total aerosol number (that is, zeroth moment) and mass (that is, first moment) concentrations for each species in 15 size bins ranging from 3 nm to 10 μm in dry diameter[22]. The mass-based model includes nitrate whereas the sectional model does not (it includes sulphate, sea salt, internally mixed elemental carbon, externally mixed elemental carbon, hydrophilic organic matter, hydrophobic organic matter, mineral dust, and aerosol–water, in 135 size-resolved aerosol tracers plus three bulk aerosol-phase species and five bulk gas-phase species). Although these two models do not encompass the full breadth of model uncertainties (for example, they share the same convection scheme), they nevertheless differ markedly in the processes and complexity of their aerosols and we therefore believe that these models provide a good initial indication of uncertainty in the aerosol responses.

Health impacts. Health impacts of surface pollution changes are calculated using established methodologies. For $PM_{2.5}$, all aerosols are evaluated at 0.5° by 0.5° resolution using the internal tracer gradients within the larger model grid boxes[23] for the mass-based model (2° by 2.5° resolution is used for the microphysical model), and primary aerosols are also downscaled on the basis of population density[24] for both models. Change in premature deaths is always calculated as

$$\Delta M = M_b \times P \times \mathrm{AF}$$

where M is the number of premature deaths due to $PM_{2.5}$, M_b is the cause-specific baseline mortality rate[25], P is population, and AF is the attributable fraction of deaths due to $PM_{2.5}$. AF can be expressed in terms of the relative risk (RR):

$$\mathrm{AF} = (\mathrm{RR} - 1)/\mathrm{RR}$$

Our baseline case, hereafter CRF_{base} (refs 10,26), uses a log-linear relationship between $PM_{2.5}$ exposure and AF:

$$\mathrm{AF} = 1 - \exp(-\beta \Delta C)$$

where β is the CRF slope and ΔC is the $PM_{2.5}$ concentration change. Starting from the American Cancer Society estimates of RR per $10\ \mu g\,m^{-3}$ increase in $PM_{2.5}$ (ref. 27), and incorporating evidence for 80% higher CRFs based on expert elicitation[28] as in ref. 10, we use β of $(\ln(1.14)/10)\times 1.8$ for lung cancer and $(\ln(1.09)/10) \times 1.8$ for cardiovascular and respiratory disease. The CRF slopes in this case correspond to 2.4% and 1.6% increases per microgram per cubic metre of $PM_{2.5}$ for lung cancer and for cardiovascular plus respiratory disease, respectively. That case is probably the most fitting for the US as epidemiological studies indicate that the CRF slope is linear at fairly low concentrations up to $\sim 40\ \mu g\,m^{-3}$, and US $PM_{2.5}$ levels are typically within that range[29,30], and the base case slopes were in fact derived from US studies of exposure to ambient pollution levels.

The CRF_{high} calculation incorporates a reduction in the CRF slope at higher exposure levels but an increase at lower levels[31], using the log of the $PM_{2.5}$ concentration with slopes of 0.2794 per $\Delta(\ln C)$ for cardiovascular and respiratory disease and 0.4180 per $\Delta(\ln C)$ for lung cancer[10,32]. The CRF_{low} calculation is based on epidemiological studies of the response to both extremely high $PM_{2.5}$ from cigarettes (direct and second-hand) as well as ambient pollution[33,34]. Cardiovascular $\mathrm{RR} = 1 + 0.2685\ (\mathrm{Inh} \times C)^{0.2730}$, where Inh is the inhalation rate ($18\ m^3\ d^{-1}$) and C is the annual average of daily $PM_{2.5}$ concentration ($d\ mg\ m^{-3}$) for control or experiment so that $\mathrm{Inh} \times C$ represents exposure (times $1\ mg^{-1}$ to become unitless)[34]. Similarly, RR for lung cancer is $1 + 0.3195(\mathrm{Inh} \times C)^{0.7433}$. Respiratory diseases are not included in this variant.

Note that all $PM_{2.5}$ components are treated equally, as data on the role of individual species are not considered conclusive (for example, by the US EPA (Environmental Protection Agency) or the WHO (World Health Organization)), but there is some evidence for differential impacts associated with different pollutants or different sources. For example, some studies have found approximately three times greater RR from mobile sources than from coal combustion sources[35,36]. However, the importance of various components or source categories seems to vary with the end points assessed, and may also depend on particle sizes, geographic location and season, with most authors concluding that associating risk with total $PM_{2.5}$ remains the current best practice[37].

Ozone–health impacts are based on the long-term relative risk from an American Cancer Society US study associating ozone with premature death from respiratory disease[38]. The RR has a value of 1.04 per 10 ppb increase in the maximum 6-month average of the 1-h daily ozone maximum[10]. An alternative calculation uses the risk due to short-term exposure[34], which assigns most impacts to increased cardiovascular disease using a RR of 1.11 for a 10 ppb increase in 24-h ozone concentrations based on a meta-analysis[39]. For comparison, the worldwide 6-month average of the 1-h daily maximum is about 33% greater than the 24-h ozone averaged over the course of a year in our models.

Owing to data limitations, the calculation uses baseline mortality rates for all people aged 15 and older whereas the CRF was measured for people aged 30 and over; hence, baseline mortality is very slightly too low. In general, this bias is expected to be small compared with the differences across CRFs. Population data for all people aged 30 or older for 2030 are used for all health calculations, and are based on gridded projections for 2015 (ref. 40) scaled at the country level according to projected changes under a medium fertility scenario[41].

For comparison, total present-day US premature deaths due to ambient anthropogenic air pollution are 114,000 (46,000–216,000) based on our modelling. An analysis using a very high-resolution model for the US found 53,000–208,000 premature deaths in their main analyses[15], a range very consistent with our estimates (although uncertainties in defining the natural portion of pollutants mean that very close agreement may be partly coincidental). Total worldwide premature deaths due to ambient $PM_{2.5}$ are 3.6–4.3 million yr^{-1}, (CRF_{base} and CRF_{high} calculations), consistent with the 2015 estimate by the World Health Organization of 3.7 million yr^{-1}.

Valuation. Health valuations use the US EPA's methodology updated to 2010.

Base VSL (value of a statistical life) = US$7.5 million $\times$ $(1.02^{(\mathrm{year}-2010)})$, where 1.02 represents assumed 2% yr^{-1} inflation. All values, however, are given in 2007 US$ (as in ref. 12).

Although most impacts occur within the US, values were weighted at the national scale according to the income levels in different countries. World Bank data on national GDP per capita for 2007 (in 2005 US$) were used after being converted to the list of countries from the WHO Global Burden of Disease. Although all countries were included, most of the $PM_{2.5}$-related impacts are in North America (and those dominate the overall health impacts), but the ozone-related impacts extend broadly over the Northern Hemisphere. The population-weighted world average value was used for the few small countries without data. Income elasticity was set to 0.4 as in ref. 24 and as recommended by the US EPA; hence, valuation of lives is based on local available funds and hence greater amounts that societies are willing to pay to avoid risk with increasing income (not greater inherent worth of lives in wealthier nations). This is implemented using:

$$\mathrm{VSL} = (\text{base VSL}) \times (\mathrm{GDP(N)}/\mathrm{GDP(US)})^{0.4}$$

Although use of a higher elasticity may be better for international comparisons, our valuations are only marginally sensitive to this value given that the preponderance of impacts is within the US. SCAR valuations include uncertainty ranges representing 95% confidence levels.

References

17. Schmidt, G. A. *et al*. Configuration and assessment of the GISS ModelE2 contributions to the CMIP5 archive. *J. Adv. Model. Earth Syst.* **6,** 141–184 (2014).
18. Shindell, D. T. *et al*. Interactive ozone and methane chemistry in GISS-E2 historical and future climate simulations. *Atmos. Chem. Phys.* **13,** 2653–2689 (2013).

19. Shindell, D. T. *et al*. Radiative forcing in the ACCMIP historical and future climate simulations. *Atmos. Chem. Phys.* **13,** 2939–2974 (2013).
20. Forster, P. *et al*. in *Climate Change 2007: The Physical Science Basis* (eds Solomon, S. *et al*.) Ch. 2 (IPCC, Cambridge Univ. Press, 2007).
21. Myhre, G. *et al*. in *Climate Change 2013: The Physical Science Basis* (eds Stocker, T. F. *et al*.) Ch. 8 (IPCC, Cambridge Univ. Press, 2013).
22. Lee, Y. H., Adams, P. J. & Shindell, D. T. Evaluation of the global aerosol microphysical ModelE2-TOMAS model against satellite and ground-based observations. *Geosci. Model Dev.* **8,** 631–667 (2015).
23. Prather, M. J. Numerical advection by conservation of second-order moments. *J. Geophys. Res.* **91,** 6671–6681 (1986).
24. Shindell, D. *et al*. Simultaneously mitigating near-term climate change and improving human health and food security. *Science* **335,** 183–189 (2012).
25. World Health Organization *Death Estimates for 2008 by Cause for WHO Member States* (WHO Department of Health Statistics, 2011).
26. Anenberg, S. C., Horowitz, L. W., Tong, D. Q. & West, J. J. An estimate of the global burden of anthropogenic ozone and fine particulate matter on premature human mortality using atmospheric modeling. *Environ. Health Perspect.* **118,** 1189–1195 (2010).
27. Pope, C. A. *et al*. Lung cancer, cardiopulmonary mortality, and long-term exposure to fine particulate air pollution. *JAMA* **287,** 1132–1141 (2002).
28. Roman, H. A. *et al*. Expert judgment assessment of the mortality impact of changes in ambient fine particulate matter in the US. *Environ. Sci. Technol.* **42,** 2268–2274 (2008).
29. Krewski, D. *et al*. *Research Report* (Health Effects Institute, 2009).
30. Laden, F., Schwartz, J., Speizer, F. E. & Dockery, D. W. Reduction in fine particulate air pollution and mortality: extended follow-up of the Harvard Six Cities study. *Am. J. Respir. Crit. Care Med.* **173,** 667–672 (2006).
31. Pope, C. A. III *et al*. Cardiovascular mortality and exposure to airborne fine particulate matter and cigarette smoke: shape of the exposure-response relationship. *Circulation* **120,** 941–948 (2009).
32. Cohen, A. J. *et al*. *Comparative Quantification of Health Risks* (World Health Organization, 2004).
33. Pope, C. *et al*. Lung cancer and cardiovascular disease mortality associated with ambient air pollution and cigarette smoke: shape of the exposure-response relationships. *Environ. Health Perspect.* **119,** 1616–1621 (2011).
34. Marlier, M. *et al*. El Nino and health risks from landscape fire emissions in southeast Asia. *Nature Clim. Change* **3,** 131–136 (2013).
35. Laden, F., Neas, L., Dockery, D. & Schwartz, J. Association of fine particulate matter from different sources with daily mortality in six US cities. *Environ. Health Perspect.* **108,** 941–947 (2000).
36. Janssen, N. A. H. *et al*. Black carbon as an additional indicator of the adverse health effects of airborne particles compared with PM10 and $PM_{2.5}$. *Environ. Health Perspect.* **119,** 1691–1699 (2011).
37. Adams, K., Greenbaum, D. S., Shaikh, R., van Erp, A. M. & Russell, A. G. Particulate matter components, sources, and health: systematic approaches to testing effects. *J. Air Waste Manage. Assoc.* **65,** 544–558 (2015).
38. Jerrett, M. *et al*. Long-term ozone exposure and mortality. *New Engl. J. Med.* **360,** 1085–1095 (2009).
39. Bell, M. L., Dominici, F. & Samet, J. M. A meta-analysis of time-series studies of ozone and mortality with comparison to the national morbidity, mortality, and air pollution study. *Epidemiology* **16,** 436–445 (2005).
40. CIESIN/FAO/CIAT *Gridded Population of the World: Future Estimates, 2015* (*GPWv3*)*: Population Grids* (NASA Socioeconomic Data and Applications Center, 2005); http://sedac.ciesin.columbia.edu/gpw
41. United Nations *United Nations World Population Prospects: The 2010 Revision* (UN Department of Economic and Social Affairs, 2011).